A Density Functional Embedded Cluster Study of Proposed Active Sites in Heterogeneous Ziegler−Natta Catalysts

Michael Seth,[†] Peter M. Margl,[‡,§] and Tom Ziegler*[,†]

Department of Chemistry, University of Calgary, University Drive 2500, Calgary AB T2N-1N4, Canada, and Eastman Chemical Company, Box 511, Kingsport, Tennessee 37664

Received March 22, 2002; Revised Manuscript Received July 1, 2002

ABSTRACT: A number of proposed models of the active sites in $TiCl_4/MgCl_2$ heterogeneous Ziegler−Natta catalysts are examined using density functional methods. Using a number of different models for the surface, the sites formed when unreduced $TiCl_4$ is adsorbed onto $MgCl_2$ are predicted to be unstable. In contrast, $TiCl_3$ and $TiCl_2$ are found to bind strongly to $MgCl_2$. Alternative models of the surface where one or all of the Mg atoms is replaced with Ti(II) give larger binding energies for $TiCl_4$. Each step of the ethylene polymerization reaction is considered for each of the site models that are expected to be active. Two possible termination mechanisms, chain transfer to the monomer and β-hydrogen elimination, are also examined. The sites formed from $TiCl_4$ bind ethylene more weakly than those formed from $TiCl_3$. No particular trends with respect to the type of site are found for the barrier to insertion, but the direction of approach of the ethylene molecule is important. The β-hydrogen elimination termination mechanism is predicted to be much less important than chain transfer to the monomer. From a comparison of ethylene insertion and termination barriers, the $TiCl_3$-based sites on the $TiCl_2$ surface and the $TiCl_3$-based Corradini site on $MgCl_2$ are shown to be very poor catalysts while the others, in particular the $TiCl_3$-based edge site on $MgCl_2$, appear to be more promising models of the actual active sites.

1. Introduction

The classical Ziegler−Natta process has been for a number of years the most important industrial method for the production of polymers from α-olefins.[1,2] It is a versatile process, capable of being run at low temperatures and pressures and in a variety of conditions such as gas phase, solution, or in a slurry. The polymers produced are relatively low in chain length and show wide molecular weight distributions, particularly in comparison with the polymers produced by homogeneous single site catalysts. The activity of the earliest Ziegler−Natta catalysts was unacceptably low. In the late 1960s it was found that if $TiCl_4$ was reacted with active $MgCl_2$, then the properties of the catalyst produced were much improved. $TiCl_4/MgCl_2$ catalysts and the many variations thereof are today the most commonly used heterogeneous Ziegler−Natta catalysts.

Despite their obvious importance, many aspects of classical Ziegler−Natta catalysts are largely unknown. Important properties such as the structure of the active sites, the role of the support, and the differences between the activity of the transition metal in various oxidation states are poorly understood. So little is known about these catalysts because of the difficulties inherent in studying a low concentration active site that is in a relatively disordered environment. In addition, most conventional surface analysis methods run into problems due to the insulating properties of $MgCl_2$ which leads to charge buildup.

Theoretical methods provide an attractive alternative. A number of calculations studying some form of heterogeneous Ziegler−Natta catalyst with Ti as the main component of the active site have been published.[3−19] While these calculations have provided significant insight into the nature of the catalysts, they have not as yet resolved all difficulties. There is still no general agreement on the structure of the active sites or their stability. Recent studies have been more systematic in their treatment of possible active sites,[10,16,17] and ref 10 in particular considers a number of titanium chlorides species adsorbed onto $MgCl_2$. A comprehensive survey of polymerization at the various active sites has yet to be done, however.

In this study we attempt to resolve some of these problems. The particular catalyst that will be considered is the $TiCl_4/MgCl_2$ catalyst already mentioned. Our major goal is to try and determine which of the proposed structures of the active site are most likely to correctly describe the actual active site or sites. This will be achieved in two steps. In the first, the stability and structures of titanium chlorides on $MgCl_2$ will be considered, much in the spirit of ref 10. In the second half of this paper calculations describing the polymerization mechanism at each of the active sites will be outlined. A comparison of the results of these calculations with what is known about the true catalyst will allow the range of possible active site models to be further refined.

Present ideas about the structure of the active sites in classical Ziegler−Natta catalysts generally start from the geometry of crystalline $MgCl_2$ and what is obtained when it is cut along particular planes.[12,20,21] $MgCl_2$ has a layer structure where layers of Mg are sandwiched between two layers of Cl in a cubic close-packed manner. In the thermodynamically most stable α-form the Cl−Mg−Cl triple layers repeat in a ABC ABC... sequence. Other known structures are the β- and γ-forms which have a AAA... repeating sequence and a disordered arrangement, respectively. In each case the Mg ions are six-coordinate and fill half of the available octahedral sites. The Cl ions are all three coordinate and occupy

[†] University of Calgary.
[‡] Eastman Chemical Company.
[§] Present address: Computing, Modeling and Information Sciences, The Dow Chemical Company, 1702 Bldg., Midland, MI 48674.

10.1021/ma0204554 CCC: $22.00
Published on Web 08/30/2002

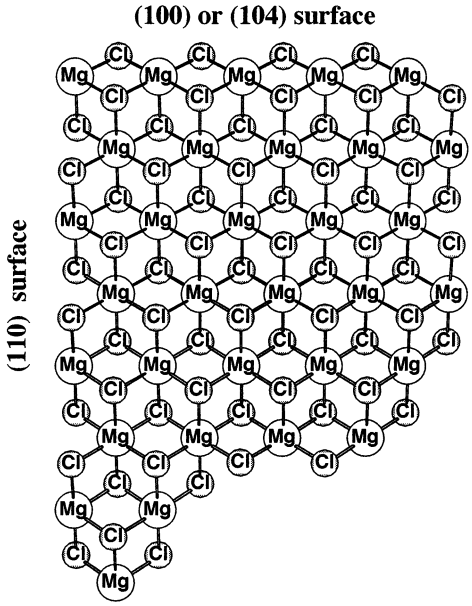

Figure 1. A portion of one $MgCl_2$ triple layer looking down on the (001) surface.

all octahedral sites. A portion of $MgCl_2$ crystal is illustrated in Figure 1.

The Cl−Mg−Cl triple layers are bound to each other only weakly via van der Waals forces, and a $MgCl_2$ crystal thus can most easily cleave between adjacent Cl layers. The (001) surface exposed is composed of fully saturated Cl atoms and therefore does not provide anywhere for a $TiCl_4$ molecule to adsorb. Alternative cuts of the crystal expose unsaturated Mg atoms which are possible sites for $TiCl_4$ adsorption. In the most commonly observed cuts of $MgCl_2$ only two different types of undercoordinated Mg atom are expected to be found, one type which is five-coordinate and one which is four-coordinate. The former is found in the (100) or (104) face (see Figure 1) and the latter in the (110) face (also see Figure 1). It is believed that these undercoordinated Mg atoms are exposed in the process of catalyst creation by treatments such as ball-milling. There is some evidence that the most prevalent exposed surface that contains undercoordinated Mg atoms is the (110) face.[22] In the same study it was found that the next most common surface was rather irregular.[22] It seems likely that this irregular surface will include areas with five-coordinate Mg atoms.

Three different types of site in which a $TiCl_4$ molecule is bound to one or more undercoordinated Mg ion have been proposed in the literature.[12,20,21] The site on the surface exposing five-coordinate Mg atoms has Ti bound through two bridging chlorine atoms and directly (if weakly) to a chlorine atom making it five-coordinate (see Figure 2a). For the sake of brevity, this site will be referred to as the "slope site" where slope refers to the appearance of the $MgCl_2$ triple layer below the site. Two sites have been proposed for the surface containing four-coordinate Mg atoms. The first site was proposed by Corradini and co-workers[23,24] and will hereafter be referred to as the "Corradini site". This site also has two bridging Cl atoms, and the Ti is expected to have bonds with two Cl atoms from the surface making it six-coordinate (see Figure 2b). The second type of site that involves the four-coordinate Mg atoms again has two bridging Cl atoms, but this time they are both bonded to a single Mg atom (see Figure 2c). When originally

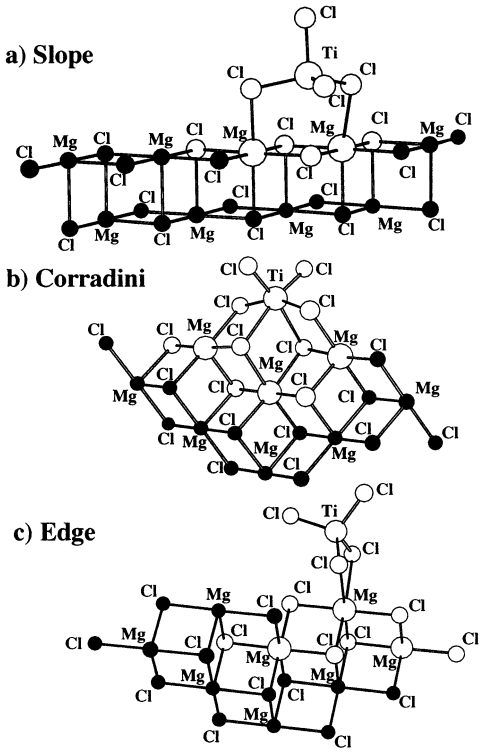

Figure 2. The three proposed sites with attached $TiCl_4$ molecule. Atoms colored black are described using molecular mechanics in the embedded cluster calculations.

proposed, it was suggested that the Ti atom also would form a bond with a surface Cl atom making it five-coordinate, but there has been some disagreement on this point.[10,15] The sites illustrated in Figure 2 are all formed by adsorbing $TiCl_4$ onto the surface of $MgCl_2$ (hereafter called $TiCl_4$-based sites). Although Ti is added to the support in the form of $TiCl_4$, there is significant experimental data that suggest that after reaction with the cocatalyst Ti may be present in the +4, +3, and +2 oxidation states.[25−30] The active sites where Ti is in a lower oxidation state were also considered and were modeled by $TiCl_3$ and $TiCl_2$ attached to the surface of $MgCl_2$. These two types of site will be referred to as $TiCl_3$-based and $TiCl_2$-based sites, respectively (see Figures 3 and 4). Thus, at this stage there are nine possible sites formed from the three possible locations that the Ti species can adsorb and the three possible oxidation states of the Ti atom.

To keep the problem to a manageable size, sites with more than one Ti atom will not be considered, and it will also be assumed that the aluminum cocatalyst is not directly involved in any reaction beyond alkylation of Ti. The effects of other possible additives such as hydrogen will also not be considered. The monomer will be limited to ethylene; i.e., issues of stereospecificty will not be dealt with. Work underway is looking at the effects of relaxing these restrictions, but for the time being we believe this represents a good starting point.

It has been found that there is often an inverse correlation between stereospecificity and productivity in Ziegler−Natta catalysts. This is interpreted to mean that there are at least two kinds of active site: one that produces isotactic or syndiotactic polymer and one that produces atactic polymer.[2] The latter kind are poisoned somehow in the treatments that produce a stereospecific catalyst. In more recent work that examines the molecular weight distribution data of the product polyeth-

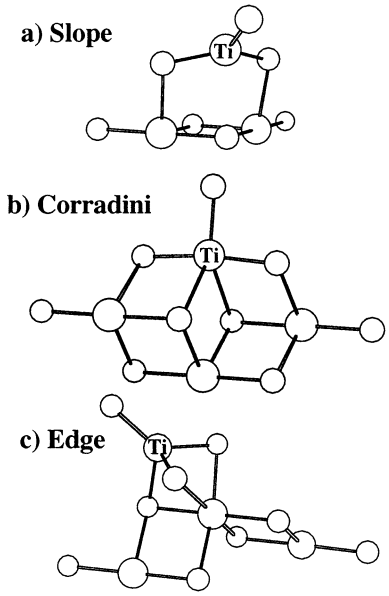

Figure 3. The three proposed sites with attached $TiCl_3$ molecule.

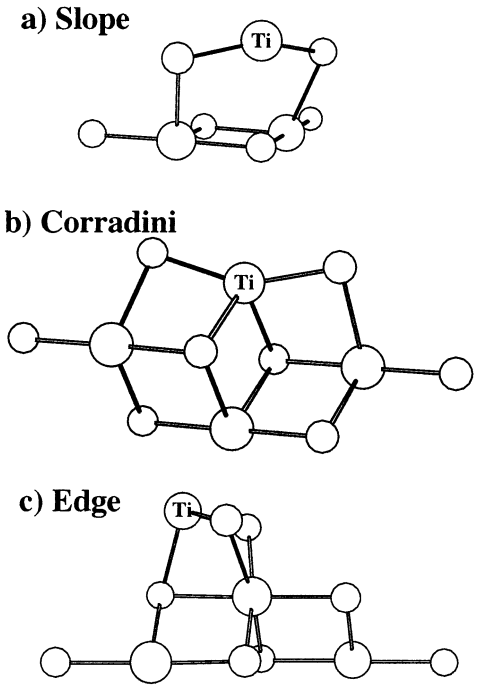

Figure 4. The three proposed sites with attached $TiCl_2$ molecule.

ylene, it was concluded that the distributions found were produced by five narrow molecular weight distributions, each of which corresponds to a single type of active site.[31,32] It therefore will not be necessary to narrow down the range of proposed possible sites to the single best in this study but rather to eliminate the sites that are poor catalysts or that do not have properties consistent with experimental results.

The most commonly accepted mechanism for the polymerization is that due to Cossee and Arlman[33−35] (Scheme 1). It is assumed that the Ti atom has at least one terminal Cl atom which can be replaced with an alkyl group by the activator. Initially, the resting state of the site consists of a Ti on the surface with the attached alkyl group R and a vacant site in its coordination sphere. An α-olefin monomer occupies the vacancy

Scheme 1

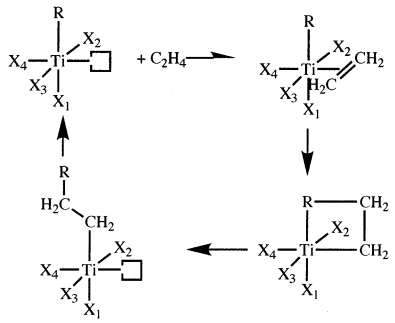

and forms a π-complex with the Ti atom. It then inserts into the Ti−R bond via a cyclobutane-like four-membered transition state, thereby increasing the polymer chain length by two carbon atoms and regenerating the resting state. There have been some modifications to this mechanism, most notably that by Brookhart and Green[36] in which the insertion step is assisted by an agostic interaction between the Ti and an α-hydrogen.

2. Computational Details

All calculations were performed using the gradient corrected density functional formed by the combination of the exchange correction given by Becke[37] and the correlation correction of Perdew[38] with the Vosko, Wilk, and Nusair parametrization of the electron gas.[39]

The $MgCl_2$ support was described using both cluster (finite) and periodic (infinite) models. The ADF program package[40−44] was used for the cluster calculations employing in most cases an embedded cluster or quantum mechanics/molecular mechanics (QM/MM) approach. The influence of the part of the surface described using MM was included only through van der Waals type terms. That is, no polarization of the wave function by the environment is included (mechanical embedding). Since $MgCl_2$ is an ionic crystal, no dangling covalent bonds are created and therefore no capping or link atoms are necessary. Which atoms are treated using QM and which are treated using MM are indicated in Figure 2. For the sake of clarity, the MM atoms will not be shown in later figures. The total cluster sizes are Mg_9Cl_{18} for the slope site (Mg_2Cl_4 QM in the QM/MM) and Mg_8Cl_{16} for the Corradini and edge sites (Mg_3Cl_6 QM in the QM/MM). These clusters are quite small, in terms of both the part described using QM and the part described using MM. Since the surfaces are part of an ionic solid, it should be possible to describe them using relatively small QM clusters.[45] The appropriateness of the QM part chosen here will be demonstrated shortly. A small MM part was chosen because for the present study only the immediate neighborhood of the active site is of interest, and the effects of other species adsorbed nearby on the surface were not considered.

The $TiCl_2$ surface was described with only the embedded cluster model in all cases. The cluster sizes and QM/MM definitions used were identical to those of $MgCl_2$.

The $TiCl_4$-based sites on $MgCl_2$ were described using spin-restricted wave functions, and unrestricted calculations were used in all other cases. The Ti in $TiCl_3$ and $TiCl_2$ environments were assumed to have one and two unpaired electrons, respectively.

The periodic calculations were performed using two different programs. BAND, which is also part of the ADF package,[43,46] was used to perform atomic centered basis set calculations. Because of the high cost of the

BAND calculations, it was only possible to include periodicity in one dimension. Therefore, the effects of adjacent $MgCl_2$ triple layers were not included. The supercell parameters in the one dimension for the surfaces including exposed five- (the 100 or 104 cut of $MgCl_2$) and four-coordinate (the 110 cut) Mg atoms were 14.5928 and 12.4569 Å, respectively. The second type of periodic calculation was based on Blöchl's implementation of the projector augmented-wave (PAW) method.[47] The PAW approach, as a type of Car−Parinello molecular dynamics calculation,[48] uses plane-wave basis sets and therefore must be periodic in three dimensions. The cell used to describe the surface with exposed four-coordinate Mg atoms was monoclinic with sides 12.1048, 12.2661, and 18.3000 Å and angle 76.13°. An orthorhombic cell was used for the surface with exposed five-coordinate Mg atoms. The parameters of this cell were 14.5928, 14.3704, and 23.0000 Å. The particular cut of $MgCl_2$ chosen to be described by this slab was the relatively flat (104) cut.

Very similar basis sets were used in the cluster and BAND calculations For the Ti of the active site a valence triple-ζ Slater type orbital (STO) was applied while for the Mg, Cl, C, H, and surface Ti atoms double-ζ basis sets were used with the exception that the 3d shell of the Ti is described with a triple-ζ set. In addition, the Mg, Cl, and C basis sets are supplemented by one 3d polarization function, and the H basis set includes a 2p polarization function. The molecular density and the Coulomb and exchange potentials were fit using an auxiliary s, p, d, f, and g set of STO functions[49] centered on each nucleus. The difference between the cluster and slab ADF basis sets lies in the treatment of the frozen core orbitals. In the case of the cluster calculations the core orbitals are described by an auxiliary set of STOs while in the BAND calculations numerical orbitals are used. The energy cutoff used to define the plane wave basis set in the PAW calculations was 30 Ry. The core definitions used in all cases were [Ne] for the active site Ti, the Cl and the Mg atoms, [He] for C, and [Ar] for the surface Ti. The van der Waals parameters of the MM parts of the embedded cluster calculations were taken from the TRIPOS force field[50] supplemented by parameters from the universal force field[51] (UFF) when TRIPOS did not include the required data.

In the embedded cluster calculations the geometry of the support was generally kept frozen at that of the bulk. The experimental parameters used to define these geometries were 3.596 Å for a_0 (Mg−Mg or Cl−Cl intralayer distance) and 17.589 Å for c_0 (interlayer distance, $MgCl_2$) and 3.561 Å for a_0 and 5.875 Å for c_0 ($TiCl_2$).[52] The geometries of the full-QM clusters were allowed to relax without restriction. The DFT method does not describe correctly the van der Waals forces between the $MgCl_2$ triple layers. Therefore, the distance between Mg layers was kept constant at the experimental value in the PAW calculations. The bottom layer of each slab was also kept frozen, but otherwise all other geometric parameters were optimized.

The convergence criteria for the cluster calculations were 0.0001 au in the energy and 0.001 au $Å^{-1}$ or au rad^{-1} in the gradient. The integration parameter used in the cluster calculations was 5.0 in most cases and 6.0 for frequency analyses. Since they were only single point calculations, the BAND computations only required an integration parameter of 4.0.[40]

Table 1. Binding Energies of $TiCl_x$ Species to $MgCl_2$ Surfaces[a]

adsorbed species	site type	E_B	adsorbed species	site type	E_B
$TiCl_4$	slope	7.3	$TiCl_3$	edge	20.6
$TiCl_4$	Corradini	8.1	$TiCl_2$	slope	24.9
$TiCl_4$	edge	5.6	$TiCl_2$	Corradini	42.0
$TiCl_3$	slope	20.0	$TiCl_2$	edge	22.2
$TiCl_3$	Corradini	18.2			

[a] Energies in kcal/mol.

Binding energies were typically calculated as the difference between the bound system (e.g., an active site with a complexed ethylene molecule) and the sum of the components (an isolated ethylene molecule and the site in its resting state). The exceptions to this are any energies calculated using PAW. In this case the binding energies were calculated as the difference in energy between the bound system and the same system but with the binding molecule removed to a distance of at least 5 Å.

3. Active Site Stability

To begin with, the binding energies (E_b) of $TiCl_4$, $TiCl_3$, and $TiCl_2$ to $MgCl_2$ in the three sites described in section 1 were calculated using the embedded cluster model of the surface (Table 1). The binding energies of the $TiCl_4$ molecules stand out in particular because they are so small—less than 10 kcal/mol for all three sites. If an ensemble of molecules are to stick to a surface to any great extent, they must exhibit not only a positive binding energy but this binding energy must be large enough to overcome an entropic barrier due to the loss of translational and rotational degrees of freedom. To get an idea of how large the binding energies need to be for equilibrium to favor the adsorbed $TiCl_4$ over the free molecule, the change in entropy for the reaction $TiCl_4(g) \rightarrow TiCl_4$ (slope site) at 350 K was calculated. The $\omega_{i,\mathrm{vib}}$ necessary for the vibrational contributions were taken from harmonic frequency analyses. ΔS was found to be −37.2 cal/(mol K), giving a value of −13.0 kcal/mol for ΔST at 350 K. None of the $TiCl_4$ binding energies in Table 1 are this large. The change in free energy upon adsorption must therefore be about +5 kcal/mol or more, and the equilibrium in this reaction is predicted to lie heavily toward unbound $TiCl_4$ molecules.

This is a rather surprising result since the commonly accepted model of the active sites starts with $TiCl_4$ adsorbed to $MgCl_2$. Previous theoretical calculations have not been in agreement as to how large the binding energy of $TiCl_4$ to $MgCl_2$ is. Some earlier calculations gave low binding energies similar to those given here.[8,10,11] Parinello and co-workers obtained low $TiCl_4$ binding energies for the slope site but are in significant disagreement with the present results for the Corradini and edge sites where they found binding energies of 40.3 and 29.4 kcal/mol, respectively.[17] In none of the earlier studies was it noted that these low calculated binding energies call into question the basic $TiCl_4$ bound onto a $MgCl_2$ surface model of the heterogeneous Ziegler−Natta catalyst.

Given the surprising nature of this result and the disagreement among previous calculations, it was felt that it was necessary to investigate the binding of $TiCl_4$ to $MgCl_2$ more carefully. The $TiCl_4/MgCl_2$ systems were therefore studied using alternative approaches to the

Table 2. Binding Energies of $TiCl_4$ to $MgCl_2$ Surfaces Calculated Using Larger QM Clusters and Periodic Methods[a]

site type	method	E_B
slope	cluster, full QM	1.4
slope	periodic	1.0
Corradini	cluster, full QM	4.4
Corradini	periodic	7.4
edge	cluster, full QM	−0.2
edge	periodic	b

[a] Energies in kcal/mol. [b] No geometry corresponding to a bound $TiCl_4$ molecule obtained for this site.

embedded cluster approach that was applied in most of the calculations described in this paper. The extra calculations take two forms: (a) cluster calculations with a greater number of QM atoms and (b) periodic calculations.

In the cluster calculations surface models of identical size to those of the embedded cluster calculations were used, but all atoms were described quantum mechanically and the geometry of the $MgCl_2$ part was allowed to relax. The results of these calculations are given in Table 2 labeled "cluster, full QM". The binding energies obtained from the full QM calculations are a little lower than those given in Table 1. This appears to be predominantly due to the surface relaxation rather than the increase in the size of the cluster since calculations with clusters of identical size but where the $MgCl_2$ geometry is kept frozen[10] give results more similar to the embedded cluster than the full QM cluster calculations in the present work. In any case, it appears that the embedded cluster model of the surface being used is adequate and, if anything, gives binding energies that are slightly too large due to the neglect of surface relaxation.

Rather than attempt to improve the model using larger and larger clusters, it was decided to describe the system using methods with periodic boundary conditions. This approach is similar to that used earlier by Catlow and co-workers[11] and Parinello and co-workers.[17]

The final binding energies were calculated using the BAND program using geometries provided by PAW calculations. Because of the high computational cost of these calculations, only a single $MgCl_2$ triple layer was included in the unit cell. Triple layers three and six layers deep were included for the (104) and (110) surfaces, respectively, which corresponds to 12 $MgCl_2$ units in the unit cell in both cases. The use of only one triple layer is a reasonable approximation since the effect of neighboring triple layers on the binding of $TiCl_4$ to the surface should be small. A few small test calculations were carried out, and the effect of neighboring layers was found to be −1.3 and 0.2 kcal/mol for the slope and Corradini sites, respectively, confirming the above-mentioned assumption. No geometry corresponding to an edge site could be obtained since the $TiCl_4$ molecule fell off the surface. This site was considered no further in the periodic calculations, and it was concluded that these results agree with the cluster calculations that the binding energy of $TiCl_4$ in an edge site is very small.

The binding energies of these systems calculated using BAND are given in Table 1 (labeled "periodic"). The binding energy of the Corradini site is close to that derived in the embedded cluster calculations at 7.4 kcal/mol, and E_b of the slope site is somewhat smaller than the embedded cluster result at 1.4 kcal/mol.

All of the binding energies of $TiCl_4$ to $MgCl_2$ calculated by alternative methods are similar in magnitude or even slightly lower than the initial embedded cluster results. Remaining possible sources of error include the basis set superposition error (BSSE) and the error introduced by using an approximate functional, in particular the neglect of van der Waals interactions. Neither of these two errors is likely to be large enough to change the initial conclusion, and in addition, they are opposite in sign and should cancel somewhat. Thus, we must conclude that the binding energies of $TiCl_4$ to $MgCl_2$ are still in disagreement with the energies given by Parinello and co-workers. Furthermore, the conclusion reached earlier is confirmed. The sites corresponding to a $TiCl_4$ molecule adsorbed onto a $MgCl_2$ surface cannot be present in Ziegler−Natta catalysts at normal operating temperatures because the $TiCl_4$ molecules do not bind to the surface strongly enough. Finally, the good agreement between the embedded cluster and other calculations is noteworthy. This shows that the embedded cluster models chosen are a reasonable description of the surface for the purposes of the present study.

There is some experimental evidence that $TiCl_4$ does not stick to $MgCl_2$. In studies modeling the Ti/$MgCl_2$ Ziegler−Natta catalysts Magni and Somorjai were unable to get $TiCl_4$ to adsorb to $MgCl_2$ at room temperature despite attempts to maximize the number of undercoordinated Mg atoms.[53,54] They estimated a binding energy of 9.7 kcal/mol for $TiCl_4$ on $MgCl_2$ from temperature-programmed desorption (TPD) experiments,[53] in fair agreement with the values given here.

Unlike $TiCl_4$, $TiCl_3$ and $TiCl_2$ have significant binding energies in all three of the sites dealt with here. The $TiCl_3$ energies are all approximately 20 kcal/mol while for $TiCl_2$ they are all greater than 22 kcal/mol. Lin and Catlow[8] and Monaco et al.[10] have also found that $TiCl_3$ binds more strongly to $MgCl_2$ than $TiCl_4$. This is probably due to the fact that both $TiCl_3$ and $TiCl_2$ but not $TiCl_4$ have valence d electrons not yet involved in bonding which can be donated to the surface Cl atoms.

The present results seem to find that the active sites in heterogeneous Ziegler−Natta catalysts can only be derived from sites starting with $TiCl_3$ or $TiCl_2$ and not $TiCl_4$, in conflict with several studies that, through titrations,[25,55,56] polarographic analysis,[26] or EXAFS,[57,58] have detected the presence of Ti in the +4 oxidation state in Ti/$MgCl_2$ catalysts. A possible resolution to this conflict is offered by the model studies of Somorjai and co-workers. As has already been noted, Magni and Somorjai were not able to get $TiCl_4$ to adsorb to $MgCl_2$.[53,54] However, through the use of more sophisticated methods than simply sputtering a $MgCl_2$ surface (premade or during creation) they were able to create $TiCl_4$/$MgCl_2$ catalysts.[30,59] Upon analysis, it was found that, before treatment with a cocatalyst, the catalysts formed were composed of a layer of Ti(IV) on the top with Ti(II) and in some cases Ti(III) and Mg in several layers below.[30,59,60] It has also been hypothesized in earlier studies that in a more conventional catalyst production procedure Ti ions have become part of the $MgCl_2$ lattice.[61,62] All of these studies state that, as well as $MgCl_2$, possible models for the surface onto which the active sites in heterogeneous Ziegler−Natta catalysts are bound could include Ti atoms.

The crystal structures of $MgCl_2$ and $TiCl_2$ are very similar. Both have the layer structure Cl−M−Cl−Cl−

M−Cl... with the metal ions occupying half the octahedral site. The crystal parameters corresponding to the intralayer structure of $MgCl_2$ and $TiCl_2$ are also very similar.[52] The major difference is in the stacking of the Cl−M−Cl triple layers. As has already been noted, the most stable form of $MgCl_2$ has an ABC ABC... structure while $TiCl_2$ has the AAA... structure like the β-form of $MgCl_2$.

Given experimental results suggesting the presence of Ti atoms in the lattice and the similarity of the crystal structures of $MgCl_2$ and $TiCl_2$, it would seem worthwhile to consider alternative models of the catalyst surface in which one or more of the Mg ions are replaced with a Ti.

As a first test, the binding energy of $TiCl_4$ to $MgCl_2$ clusters with a single Mg replaced with a Ti atom was considered. The so-called "full QM" Mg_9Cl_{18} and Mg_8Cl_{16} clusters described earlier were used so that geometry optimizations could be performed on the hybrid clusters. In the Mg_9Cl_{18} cluster one of the five-coordinate Mg ions is replaced with Ti while in the Mg_8Cl_{16} cluster a four-coordinate Mg is replaced. Each of these surface Ti atoms was assumed to have two unpaired electrons. The $TiCl_4$ molecules were placed such that in the case of the Corradini and slope sites one Ti−Cl−Ti bridge was formed and in the case of the edge sites two such bridges were formed. The new binding energies of $TiCl_4$ were 13.5, 7.6, and 14.5 kcal/mol for the slope, Corradini, and edge sites, respectively, which can be compared with 1.4, 4.4, and −0.2 kcal/mol for the equivalent pure $MgCl_2$, full QM calculations. It seems therefore that if one Mg ion is substituted with a Ti, then $TiCl_4$ should be able to stick to the surface with a large enough binding energy to overcome entropy, at least in the cases of the slope and edge sites. It is also worth noting that the substitution of a Mg atom with a Ti atom did not lead to any significant change in the geometry of the $MgCl_2$ clusters.

There is obviously a huge number of possible sites where one, two, or several of the Mg atoms could be replaced with Ti. It is not worthwhile to consider all of these possibilities in detail. The surface model that was chosen as an example of a system where some of the Mg atoms have been substituted with Ti was that of pure $TiCl_2$. The reasons for this choice were threefold. First, given that the substitution of Mg with Ti increases the binding energy of $TiCl_4$, then the most favorable sites will be those with the maximum number of Ti atoms in the surface, a situation that should be well described by pure $TiCl_2$. Second, from the work of Magni and Somorjai there are examples of systems where several layers below the uppermost are composed purely of Ti(II).[59] Finally, this model allows the surface to be described in a simple way using embedded cluster calculations which are strictly analogous to those used for pure $MgCl_2$. Since the structures of the layers making up $MgCl_2$ and $TiCl_2$ are identical, the possible binding sites for $TiCl_2$ are identical to those already described for $MgCl_2$ and will be described using the same nomenclature.

The calculated binding energies of $TiCl_4$, $TiCl_3$, and $TiCl_2$ to the $TiCl_2$ embedded cluster surfaces are given in Table 3. All of the energies in Table 3 are significantly greater than the equivalent energies for the pure $MgCl_2$ surface and are large enough to indicate that the $TiCl_x$ molecule will remain bound to the surface of $TiCl_2$ at temperatures between 300 and 400 K. The $TiCl_3$ and $TiCl_2$ binding energies are again significantly larger than those of $TiCl_4$. Magni and Somorjai estimate an adsorption energy of 38 kcal/mol of $TiCl_4$ on $Ti_xMg_{1-x}Cl_2$,[63] which is somewhat larger than the $TiCl_4$ values from Table 3.

Table 3. Binding Energies of $TiCl_x$ Species to $TiCl_2$ Surfaces[a]

absorbed species	site type	E_B	absorbed species	site type	E_B
$TiCl_4$	slope	26.9	$TiCl_3$	edge	34.2
$TiCl_4$	Corradini	24.5	$TiCl_2$	slope	63.4
$TiCl_4$	edge	27.8	$TiCl_2$	Corradini	54.6
$TiCl_3$	slope	42.5	$TiCl_2$	edge	34.3
$TiCl_3$	Corradini	42.5			

[a] Energies in kcal/mol.

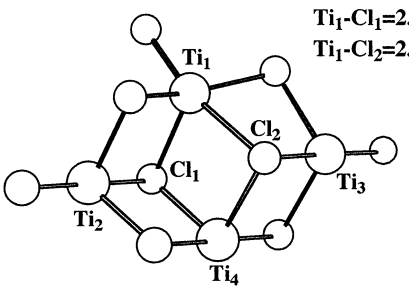

Figure 5. $TiCl_3$ at a Corradini site on $TiCl_2$.

Before turning to the polymerization process itself, a few points regarding the geometries of the site should be noted. The $TiCl_4$-based, $TiCl_3$-based, and $TiCl_2$-based sites on $MgCl_2$ are shown in Figures 2, 3, and 4, respectively. For the sake of brevity, the sites on the $TiCl_2$ surface will not be shown. With one exception, the only noteworthy difference between the two sets of structures is the bridging Cl to surface metal distances which are shorter by between 0.05 and 0.15 Å when the surface is $TiCl_2$. The exception is the $TiCl_3$-based Corradini site. This site on $TiCl_2$ is shown in Figure 5. In ref 10 it was found that $TiCl_3$ in the Corradini site does not bind symmetrically with the result that one of the Ti to surface Cl bond lengths is significantly shorter than the other. In contrast, in the present calculations it is found that $TiCl_3$ binds symmetrically in the Corradini site of $MgCl_2$. To confirm this result, the geometry of this site was reoptimized with the $MgCl_2$ described fully quantum mechanically and all geometric parameters allowed to relax. The more symmetrical site was again obtained. Interestingly, the $TiCl_3$ Corradini site with $TiCl_2$ as the surface was found to be asymmetric (Figure 5). The second point of interest with regard to the geometries concerns the $TiCl_4$ edge site. Boero et al. found that this site has two Ti−Cl−Mg bridges and a Ti to surface Cl bond giving a five-coordinate Ti atom.[15] In contrast, Monaco et al. found that no Ti to surface Cl bond was formed, and the Ti was four-coordinate instead.[10] In this work a four-coordinate site is obtained with both the $MgCl_2$ and $TiCl_2$ surfaces. The Ti to surface Cl bond is present in the $TiCl_3$-based and $TiCl_2$-based sites.

4. Mechanistic Studies

As was noted earlier, the mechanism of the polymerization reaction occurring on the surface of classical Ziegler−Natta type catalysts is believed to be that proposed by Cossee and Arlman.[33−35] In this section calculations dealing with each of the four steps in the

process—resting state, bound monomer, transition state of the insertion step, and products—will be described. In addition, some possible termination steps will also be investigated.

Modeling the surface of the catalyst as $TiCl_2$ has an unfortunate side effect. Each of the surface Ti atoms has two unpaired electrons which interact very weakly with the unpaired electrons on the other Ti atoms. In such a situation it is often very difficult to obtain converged wave functions using a single determinant based approach like that used here. In most cases convergence was eventually achieved, but in a number of others no converged wave function could be obtained. The most difficult case was the $TiCl_4$-based edge site which gave no converged results. The only other calculation that could not be completed was that involving the termination reaction of the $TiCl_3$-based edge site. To get around these difficulties, a third model of the surface unfortunately had to be used. In this model the surface is chosen to be $MgCl_2$ with a single Mg replaced with a Ti atom much like the earlier test calculations but using the embedded cluster approach. The Mg atom that was replaced was that to which the bridging Cl atoms are attached. A few of the successful calculations were repeated with this model, and it was found to give very similar results, for the edge sight at least. From here on only the $MgCl_2$ and $TiCl_2$ surface will be referred to, but it should be kept in mind that all of the results concerning the $TiCl_4$-based edge site and the termination step at the $TiCl_3$-based edge refer to calculations using a single Ti atom in the surface rather than a pure $TiCl_2$ surface.

Two different surface models ($MgCl_2$ and $TiCl_2$), three different site geometries (slope, Corradini, and edge), and three molecules to be adsorbed to the surface ($TiCl_4$, $TiCl_3$, and $TiCl_2$) have been considered. All possible combinations of these possibilities gives a total of 18 proposed sites. Even though this study seeks to make a survey of all sites involving one Ti atom, it was not necessary to consider the polymerization and termination processes of all 18 sites. The following sites can be excluded from further discussion: the sites formed by $TiCl_2$ adsorbed on either surface type and the Corradini site formed by $TiCl_4$ and either a $MgCl_2$ or a $TiCl_2$ surface. The $TiCl_2$-based sites will not be discussed for the simple reason that they are very unlikely to be activated by the cocatalyst. The Cossee−Arlman mechanism requires a terminal Cl atoms bonded to a Ti atom which can be replaced with an alkyl group. From Figure 4 it is obvious that the only Cl atoms bonded to Ti in the $TiCl_2$-based sites are bridging Cl atoms. It is expected that the energy barrier to any substitution reaction involving these atoms would be extremely high. It should be noted that particular Ti(II) species adsorbed onto $MgCl_2$ have been shown to be good catalytic centers[64] but that the structure of these sites are very different from those considered here. The $TiCl_4$-based Corradini sites are not considered because the Ti atom in this site is six-coordinate leaving no vacant coordination site into which a monomer can find its way, thereby precluding any polymerization reaction.

The neglect of these eight sites leaves 10 for further investigation. Although they are unlikely to be present, the slope and edge sites formed by the adsorption of $TiCl_4$ on $MgCl_2$ will be considered for purposes of comparison.

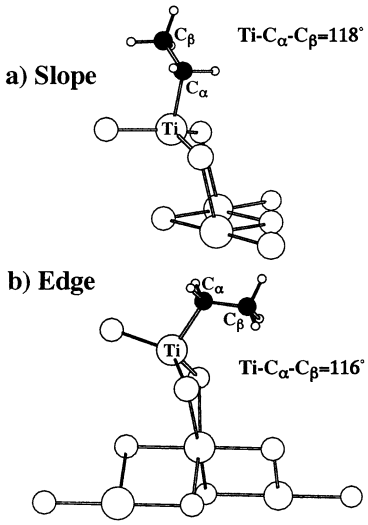

Figure 6. Resting state geometries of the $TiCl_4$-based sites.

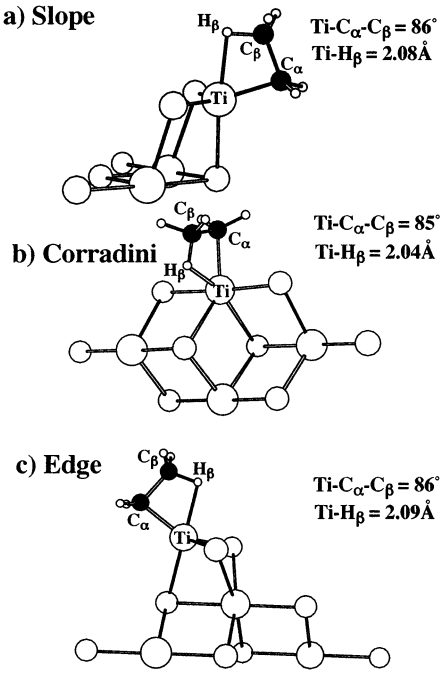

Figure 7. Resting state geometries of the $TiCl_3$-based sites.

4.1. Resting States. The polymerization mechanism begins with the activated site waiting for the approach of a monomer. This resting state was modeled by replacing one of the site's terminal Cl atoms with an ethyl group. The optimized geometries of the $TiCl_4$ and $TiCl_3$ on $MgCl_2$ sites are shown in Figures 6 and 7. Much like the unactivated sites, the sites on $TiCl_2$ are similar to the equivalent $MgCl_2$ sites and are not shown for the sake of brevity. This policy will be followed throughout except in the few cases where qualitatively different geometries were obtained for equivalent sites on different surfaces.

In general, the substitution of a Cl atom with an ethyl group has little effect on the geometry about the Ti atom. The $TiCl_3$-based sites all show a $C^{\beta}-H$ agostic interaction with $Ti-C^{\alpha}-C^{\beta}$ bond angles of approximately 85° and Ti−H distances of between 2.05 and 2.10 Å. An idea of the strength of the $C^{\beta}-H$ agostic was derived from comparisons with calculations where the starting configuration of the ethyl group was not well-suited for the formation of any $C^{\beta}-H$ agostic interaction.

Table 4. Alkylation Energies of $TiCl_4$ and $TiCl_3$ Bound to the $MgCl_2$ and $TiCl_2$ Surfaces and Binding Energies of $TiCl_xEt$ (x = 2, 3) Species to Those Surfaces[a]

absorbed species	site type	E_A[b]	E_B[c]
$MgCl_2$ surface			
$TiCl_4$	slope	−8.6	10.7
$TiCl_4$	edge	−8.9	9.3
$TiCl_3$	slope	−4.2	26.8
$TiCl_3$	Corradini	−6.1	26.9
$TiCl_3$	edge	−1.9	24.9
$TiCl_2$ surface			
$TiCl_4$	slope	−3.2	25.6
$TiCl_4$	edge	−3.7	26.3
$TiCl_3$	slope	−1.2	42.9
$TiCl_3$	Corradini	0.6	40.0
$TiCl_3$	edge	1.5	35.2

[a] Energies in kcal/mol. [b] Alkylation energy, reaction 1. [c] Binding energy.

In some cases the geometry optimizer was still able to find the lower energy minimum corresponding to a structure with a β-agostic interaction present, but in the majority a minimum was found where no such interaction existed. Such minima were of the order of 3 kcal/mol higher in energy than the equivalent optimized geometry with a $C^{\beta}-H$ agostic interaction present. The lowest energy structures for the $TiCl_4$-based sites do not have the $C^{\beta}-H$ agostic bond present. Minima where such bonds where present were found but were between $^1/_2$ and 2 kcal higher in energy than the structures without any $C^{\beta}-H$ agostic bond.

A number of other conformations of the ethyl group beyond those shown in Figures 6 and 7 were examined to ensure that the global minima were found. The reported structures were those lowest in energy, but most of the other conformations examined were only slightly (at most about 5 kcal/mol) higher in energy. Thus, the growing polymer chain is not rigidly fixed in the positions indicated but should be able to move around in the coordination sphere of the Ti atom as the situation demands.

For the purposes of this study the cocatalyst was assumed to be $AlEt_3$. This is obviously something of an approximation as these aluminum compounds generally exist as dimers, but it is sufficient for the present work. The energy of the alkylation reaction

$$Ti-Cl + AlEt_3 \rightarrow Ti-Et + AlClEt_2 \qquad (1)$$

for each of the sites are given in Table 4. The alkylation energies are all fairly close to zero and are the more exothermic for the $TiCl_4$ sites and the sites on $MgCl_2$. This reaction has been studied in some detail by Puhakka, Pakkanen, and Pakkanen.[13]

The binding energies of $TiCl_3Et$ and $TiCl_2Et$ in most of the site/surface type combinations considered are also given in Table 4. The energies are in general higher than those of the corresponding unalkylated Ti chlorides but only by a kilocalorie or two. Thus, it would be expected that if the Ti species were to be alkylated before being exposed to the activated $MgCl_2$, then its adsorption behavior would be similar to that of the unalkylated molecule.

4.2. π-Complexes. The second step in the polymerization mechanism is the complexation of an olefin to the Ti atom of the active site. It has long been recognized that the binding of a monomer to a transition metal should be possible through donation of electron density from the olefin π-orbital into the empty metal d-orbitals as well as back-donation from these metal orbitals into the π^*-orbital of the monomer. It was believed that the shifts in electron density weakened the Ti−R bond and the monomer double bond, thereby reducing the insertion barrier.[1] Some of the earliest ab initio calculations looking at Ziegler−Natta catalysis[4] confirmed this hypothesis.

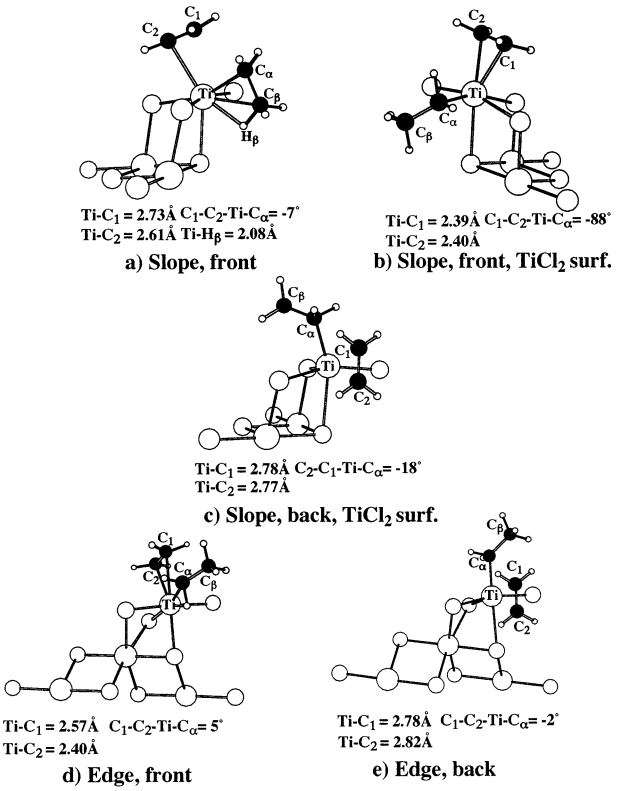

Figure 8. π-Complexes of the $TiCl_4$-based sites.

Minima corresponding to an ethylene monomer bound to the Ti atom were searched for in all of the sites still under consideration. The monomer can approach the Ti atom from two sides (labeled "front" and "back") in each case. The "front" of the slope and edge sites was taken to be the side of the Ti atom opposite from the surface. The "back" surfaces are on the opposite side of the Ti from the bridging Cl atoms and are thus actually close to perpendicular to the "front". The definitions of "front" and "back" are further clarified in Figures 8 and 9 where the optimized geometries of the olefin complexes are shown. The geometries of the π-complexes formed with the $TiCl_4$-based slope sites on $TiCl_2$ are given in Figure 8b,c because no minimum corresponding to a complex could be found for the approach of an ethylene molecule to the backside of the $TiCl_4$-based slope site on $MgCl_2$ and the two complexes where the monomer approaches from the front side (a and b) are somewhat different. No minimum corresponding to a bound olefin approaching from the front side was found for the $TiCl_4$-based edge site on $TiCl_2$ also.

The Corradini site could also be said to have a "back" and a "front" because it was found that the β-agostic interaction can be retained even with the addition of ethylene and the monomer can bind nearer to the Ti−C bond or the Ti−H bond. The former case is lower in energy and is shown in Figure 9c. These two cases will not be distinguished because the insertion reaction cannot take place when the Ti−H bond is between the

Table 5. Energies and Geometrical Parameters of the Polymerization and Chain Transfer Reactions

site type		face	E_π[c]	$E_{I(\pi)}$[d]	$E_{I(s)}$[e]	$R_{C_\alpha C_1}$[f]	$E_{T(\pi)}$[g]	$E_{T(s)}$[h]	$R_{C_\beta H}$[i]	$R_{C_1 H}$[j]
$MgCl_2$ surface										
$TiCl_4$	slope	front	−8.1	2.8	10.9	2.12	4.3	11.5	1.44	1.50
$TiCl_4$	slope	back	*b*	*b*	10.4	2.15	*b*	11.8	1.44	1.50
$TiCl_4$	edge	front	−2.0	0.0	2.0	2.34	3.0	6.4	1.46	1.50
$TiCl_4$	edge	back	1.6	3.6	2.0	2.14	6.7	6.4	1.46	1.50
$TiCl_3$	slope	front	14.3	12.5	−1.8	2.07	11.9	−1.8	1.47	1.45
$TiCl_3$	slope	back	11.4	8.2	−3.2	2.23	9.8	−1.6	1.41	1.53
$TiCl_3$	Corradini	front	11.9	8.0	−3.9	2.17	7.3	−4.6	1.43	1.48
$TiCl_3$	edge	front	14.4	11.9	−2.5	2.09	18.2	4.3	1.54	1.54
$TiCl_3$	edge	back	9.6	8.9	−0.7	2.21	15.0	4.3	1.54	1.54
$TiCl_2$ surface										
$TiCl_4$	slope	front	−4.1	3.9	8.0	2.35	6.4	10.5	1.43	1.48
$TiCl_4$	slope	back	−1.4	8.5	9.9	2.25	9.1	10.5	1.44	1.48
$TiCl_4$	edge	front	*b*	*b*	2.3	2.45	*b*	4.5	1.45	1.49
$TiCl_4$	edge	back	−1.1	1.5	2.6	2.22	2.7	4.5	1.45	1.49
$TiCl_3$	slope	front	9.9	16.1	6.1	2.08	6.5	−2.9	1.48	1.50
$TiCl_3$	slope	back	10.1	13.3	3.2	2.12	7.7	−2.7	1.46	1.52
$TiCl_3$	Corradini	front	11.0	9.4	−1.6	2.03	7.9	−3.1	1.45	1.49
$TiCl_3$	edge	front	16.1	14.8	−1.3	2.10	15.0	−1.4	1.53	1.54
$TiCl_3$	edge	back	13.4	12.9	−0.5	2.14	11.3	−1.4	1.53	1.54

[a] Energies in kcal/mol. Bond lengths in Å. [b] No geometry corresponding to a bound monomer could be found for these sites. [c] Complexation energies. [d] Ethylene insertion barrier with respect to π-complex. [e] Ethylene insertion barrier with respect separated monomer and site. [f] Distance between α-C of polymer and nearest C of ethylene in insertion transition state. [g] Hydrogen transfer barrier with respect to π-complex. [h] Hydrogen transfer barrier with respect to separated monomer and site. [i] Distance between transferring H and β-C of polymer in chain transfer transition state. [j] Distance between transferring H and nearest ethylene C in chain transfer transition state.

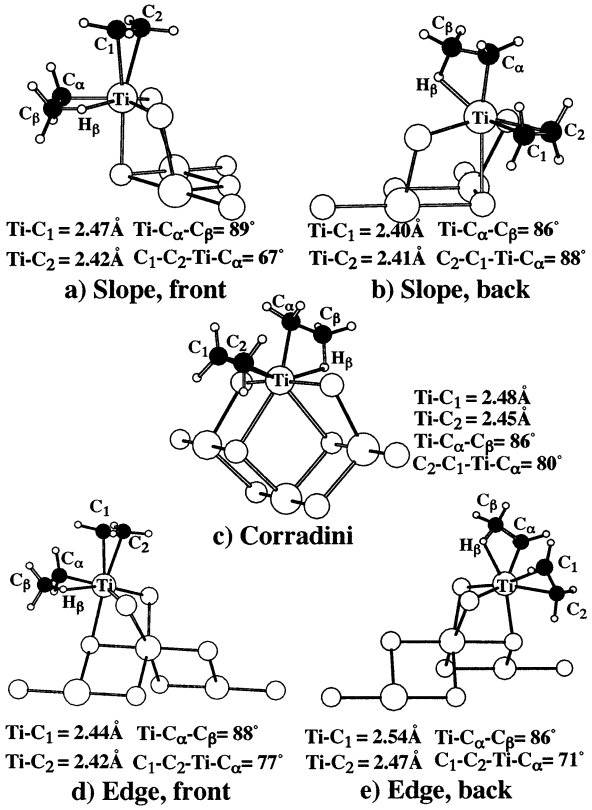

Figure 9. π-Complexes of the $TiCl_3$-based sites.

monomer and the Ti−C bond, and the chain transfer with the ethylene cannot take place when the Ti−C bond is between the ethylene and the Ti−H bond.

The calculated ethylene complexation energies (E_π) are given in Table 5. As has already been noted, no minimum corresponding to a π-complex when ethylene approaches from the back was found for the $TiCl_4$-based slope site on $MgCl_2$ or when ethylene approaches the $TiCl_4$-based edge site on $TiCl_2$. The other two π-complexes with $TiCl_4$-based slope sites are both higher in energy than the separated components. A very small positive binding energy was obtained for the $TiCl_4$ edge site on $MgCl_2$ with the monomer approaching from the back and the π-complexes of the other $TiCl_4$-based edge sites again higher in energy than the unbound ethylene system. In contrast, Parinello and co-workers[15] calculated values of E_π of greater than 40 kcal/mol for the $TiCl_4$ edge site. When propylene rather than ethylene was used as the monomer, complexation energies of 1.7 and 3.6 kcal/mol were obtained.[16]

The ethylene binding energies obtained for all the $TiCl_3$-based sites are significantly exothermic at around 10 kcal/mol. The greater binding energies of these sites in comparison with the $TiCl_4$-based sites are due to the lesser steric crowding and the additional electron density available at the metal for donation into the π^*-orbital of the monomer. Parinello and co-workers also calculated the binding energy of ethylene to a $TiCl_3$-based Corradini site on $MgCl_2$, again reporting an extremely high value of more than 45 kcal/mol. Lin and Catlow obtained more reasonable values of between 4 and 8 kcal/mol for this site but give binding energies of about 35 kcal/mol for the $TiCl_3$-based slope site.[8] Cavallo and co-workers considered a $TiCl_3$-based Corradini site and obtained 8.3 kcal/mol for the binding energy of ethylene to this site.[9]

The lowest energy geometries for each of the $TiCl_3$-based active sites (front and back coordination) in all cases give an orientation of the ethylene molecule that is not appropriate for the insertion step which would be parallel with the bond between the Ti atom and C^α in the growing polymer chain. The C−C bond of the monomer is either perpendicular to the Ti−C or at least rotated away from parallel by more than 45° (the $C_1-C_2-Ti-C_\alpha$ dihedral angles are given in Figure 9). Structures where the C−C and Ti−C bonds were parallel were optimized in a few cases and found to be 2−3 kcal/mol higher in energy than the perpendicular/staggered conformations. In most of the $TiCl_4$-based sites the ethylene C−C axis is parallel with the Ti−C bond. For several of these sites minima where the ethylene molecule is perpendicular to the Ti−C were found, but these geometries were between 1 and 4 kcal/

mol higher in energy than the corresponding parallel structure. The exception is the slope site on $TiCl_2$ when the ethylene approaches from the front (see Figure 8b) which has the ethylene molecule nearly perpendicular to the Ti−C bond like the $TiCl_3$-based sites.

While substitution of one of the terminal Cl atoms with an ethyl group had little effect on the geometry about the Ti atom, the addition of an ethylene molecule does result in nonnegligible changes in several of the active sites considered here. Perhaps the most dramatic change is in the $TiCl_4$-based edge sites. As was noted in section 3, a $TiCl_4$ molecule adsorbed at an edge site prefers to be four-coordinate rather than five-coordinate, i.e., with no Ti−Cl(surface) bond. Upon the complexation of an ethylene molecule the relative energy ordering is reversed, and the approximately octahedral six-coordinate π-complex is slightly lower in energy than the five-coordinate complex. All of the other sites which can bind ethylene molecules change in the opposite manner and show significantly increased Ti−Cl(surface) bond lengths. The ethylene C−C bond is lengthened slightly in each case as would be expected, and the Ti−R bond length is also lengthened slightly though only in most cases rather than all. The $TiCl_4$-based slope site on $MgCl_2$ with the ethylene bound to the front is also unusual in that it has a C^{β}−H agostic interaction unlike any of the other $TiCl_4$-based π-complexes or resting states. Despite several attempts, no other geometry corresponding to a bound ethylene molecule on the front side could be found for this site.

4.3. Insertion. The calculated insertion barriers (E_I) and values of $R(C_\alpha C_E)$ at the transition states that were found are given in Table 5. Energies relative to the π-complex (internal insertion energy barrier, $E_{I(\pi)}$) and separated unbound monomer ($E_{I(s)}$) are listed. The transition state structures are illustrated in Figures 10 and 11. As before, only the sites on $MgCl_2$ are shown as the geometries of the sites on $TiCl_2$ are similar. The exception to this is $TiCl_4$-based site with ethylene approaching from the front. Like the π-complexes, the insertion transition states for this site on the two surfaces are qualitatively different, and the transition state of the site on $TiCl_2$ is therefore also illustrated in Figure 10c.

The calculated internal insertion energy barriers ($E_{I(\pi)}$) of the $TiCl_3$-based sites and the insertion reactions from the back of the $TiCl_4$-based slope site on $TiCl_2$ fall in the range 8−16 kcal/mol. The remaining internal energy barriers are all less than 4 kcal/mol. Early work by Natta using a $TiCl_3$ catalyst gave an E_a of 10 kcal/mol,[65] and in a later study also involving the crystalline $TiCl_3$ catalyst Machon and co-workers obtained activation energies of between 5.0 and 8.5 kcal/mol depending on the activator used.[66] Chien and Bres considered the $TiCl_4/MgCl_2$ type of catalyst studied here and obtained activation barriers of 6.8 and 9.1 kcal/mol for their type one and type two active sites, respectively.[67]

The $E_{I(\pi)}$ in general depends of the side of the Ti atom from which the monomer approaches. In the case of the sites based on $TiCl_3$, the internal energy barriers to insertion when the ethylene molecule approaches from the "back" side are lower than the barriers to insertion when the monomer approaches from the "front" side. For the two $TiCl_4$-based sites for which π-complexes were found the trend is reversed, and the barriers to insertion from the front are lower.

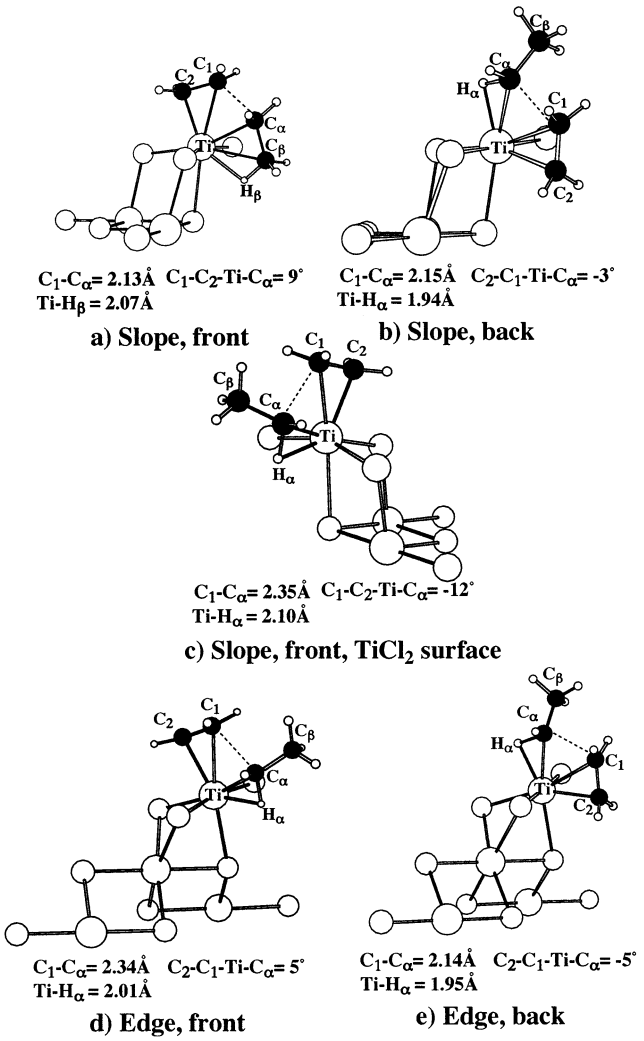

Figure 10. Insertion transition states of the $TiCl_4$-based sites.

If one considers the barriers with respect to separated monomer and active site, the distinction between the back and front approaches is much less clear as the differences between the back and front insertion barriers are smaller than for the equivalent internal energy barriers, and there is no apparent trend. Comparing the different types of sites, $E_{I(s)}$ is slightly below the energy of the separated reactants for all of the $TiCl_3$-based sites except the slope site on $TiCl_2$. The insertion barriers for the $TiCl_4$-based sites are all above the energy of the separated components, slightly in the case of the edge sites and significantly in the case of the slope sites.

Parinello and co-workers calculated the ethylene insertion barriers for the $TiCl_4$-based edge site with back coordination and the $TiCl_3$-based Corradini site obtaining about 13 and 6 kcal/mol, respectively. Catlow and co-workers give a value of 12.7 kcal/mol for a site that is geometrically similar to the $TiCl_3$-based slope site. Cavallo and co-workers obtained 8.6 and 6.6 kcal/mol for $E_{I(\pi)}$ with the polymer chain modeled as a methyl and ethyl group, respectively, in good agreement with the present value of 8.0 kcal/mol.

The geometries of the transition states all share a number of features. All of the transition states have the four-membered ringlike structure assumed by the Cossee−Arlman mechanism. The four atoms in the ring are not coplanar, however, with the dihedral angles between the Ti−R and ethylene C−C bonds all being in the range

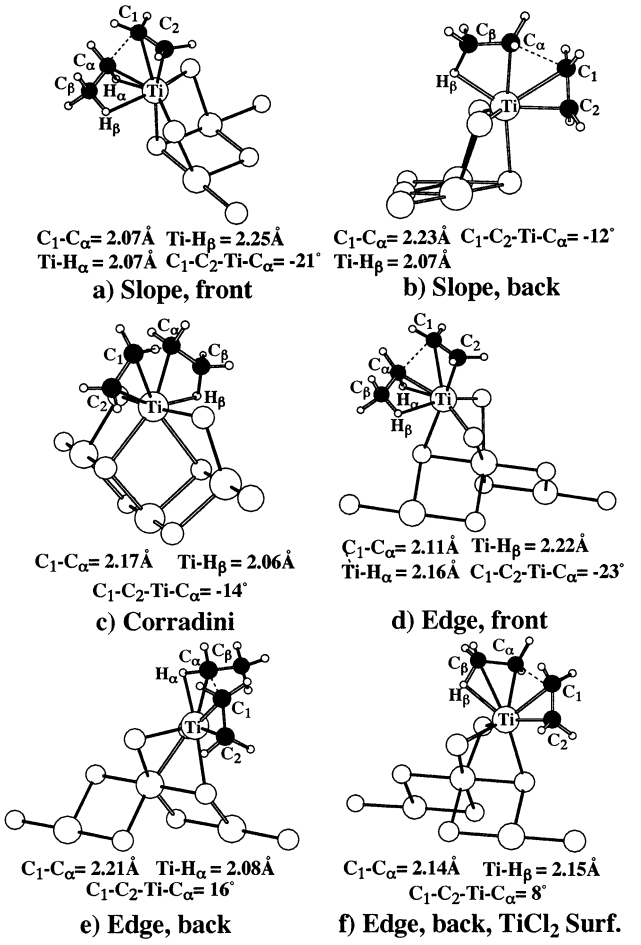

Figure 11. Insertion transition states of the $TiCl_3$-based sites.

between 5° and 21°. In all of the transition state geometries some kind of agostic H−Ti bond is present. The Ti atoms in most of the $TiCl_4$-based sites have no space for a β-H and therefore have α-agostic bonds in their transition states. The exception to this in the transition state of insertion from the front at the $TiCl_4$-based slope site on $MgCl_2$ (Figure 10a). A similar transition state structure was found for the same site on $TiCl_2$, but the energy of this structure is 3 kcal/mol higher in energy than that of the structure given in Figure 10c. We were unable to find a transition state where the β-H agostic interaction was not present. This site and the $TiCl_4$-based edge site on $MgCl_2$ with the ethylene approaches from the back are also unusual in that the transition state geometries are very similar to those of the corresponding π-complexes. Compare Figure 8a,d with Figure 10a,d. The values of $R(C_\alpha C_1)$ for the π-complexes are 2.60 and 2.46 Å for the slope and edge sites, respectively, which may be compared with 2.12 and 2.35 Å at the transition states. The internal energy barriers to insertion for these two sites are also very low (just slightly more than zero in the case of the edge site), and they both bind ethylene endothermically. It seems therefore that for these sites when the ethylene approaches from the front, it must overcome a significant barrier to complexation but that the well corresponding to the complex is very shallow and insertion (or loss of the ethylene molecule again) should be very rapid.

The behavior when the ethylene molecule approaches from the front of the $TiCl_4$-based edge site on $TiCl_2$ is similar but not identical. In this case the energy curve as a function of $R(C_\alpha C_1)$ is again very flat in the region $2.3 < R(C_\alpha C_1) < 2.6$, but in this case it is so flat that it contains no minimum corresponding to a π-complex and no maximum which would correspond to an insertion transition state. The energy and bond length of the insertion transition state for this site which are listed in Table 5 are taken from the midpoint of the flat region.

In some of the insertions involving the $TiCl_3$-based sites the Ti atom has enough space around it for both α- and β-agostic bonds to be formed although these are longer (and presumably weaker) than those in the structures where only a single agostic bond is present. The transition states of the $TiCl_3$-based sites that do not have two agostic bonds are the Corradini sites, the backside insertion of the slope site and the backside insertion of the edge site. In the first two cases the preferred orientation of the polymer chain has the C^β in the same (approximate) plane as the four atoms participating in the insertion reaction, thereby making the formation of α-agostic interactions impossible. Transition states of a similar type were found for the backside insertion at the edge site on $MgCl_2$ but were relatively high in energy because of unfavorable steric interactions with the two bridging Cl atoms bonded to the Ti of the active site. The lowest energy insertion transition states turned out to have only an α-agostic interaction much like most of the $TiCl_4$ site transition states. In contrast, the only transition state found for the same site on $TiCl_2$ had a C^β−H agostic interaction and no C^α−H agostic interaction present. Since it is somewhat different, the geometry of this transition state is given in Figure 11f.

The ethylene C−C bond lengths in each of the transition states are between 1.40 and 1.43 Å with the exception of the $TiCl_4$-based slope sites for which the bond length is about 1.39 Å. Similarly, $R(C_\alpha C_1)$ at the transition state is quite long at between 2.07 and 2.35 Å. These geometrical parameters indicate that the reaction has a fairly early transition state as the ethylene C−C bonds have stretched less that halfway from the starting value of 1.33 Å (isolated ethylene) or approximately 1.36 Å (bound monomer) to the final value of about 1.52 Å and the new C−C bonds being formed are significantly longer than 1.52 Å. An early transition state is to be expected for this reaction given that it is significantly exothermic.

4.4. Products. The product of the insertion reaction in our model system is the active site in its resting state again but with a butyl group forming the polymer chain. The total reaction energy for the insertion was in all cases calculated to be exothermic by between 24 and 26 kcal/mol.

Given that the transition states of the insertion reaction all have either an α- or β-agostic interaction the final product would be expected to have a γ- or a δ-agostic interaction immediately after insertion has taken place. The relative energies of the conformations of two sites (the $TiCl_3$-based Corradini and $TiCl_4$-based slope sites on $MgCl_2$) with δ-, γ-, and β-agostic and no agostic interactions present were evaluated, and it was found that the structure with the β-agostic interaction was lower in energy than any of the others by at least 4 kcal/mol for the $TiCl_3$-based site and that the conformation with no agostic interaction present was the lowest in energy for the $TiCl_4$-based site.

4.5. Chain Transfer. A number of termination mechanisms for the polymerization process under in-

vestigation have been proposed, including chain transfer to the monomer, dihydrogen, the aluminum cocatalyst, and spontaneous β-elimination.[2] In the present work the two mechanisms that require only the active site and perhaps a monomer molecule, i.e., spontaneous β-elimination and chain transfer with a monomer, were considered. These two mechanisms start from the resting state and the π-complex, respectively. In all calculations involving termination steps the growing polymer chain is modeled by a propyl group, the shortest possible alkyl chain in which hydrogen atoms attached to a secondary C^{β} will be present.

Spontaneous β-elimination will be discussed first. Initial attempts to find the transition state were restricted to the $TiCl_3$-based slope site on $MgCl_2$ and the $TiCl_4$-based slope site on $TiCl_2$. Difficulties arose in these calculations because in all cases the gradient along the reaction coordinate that was obtained at the optimized geometry indicated that a much shorter Ti−H bond length was required to get closer to the transition state. To help solve this problem, it was decided to calculate the properties of the product of the β-elimination, the site with a Ti−H bond, and a propylene molecule in the vicinity. Surprisingly, the optimized geometry of this system did not include a titanium hydride at all but rather corresponded to the resting state of the site with a propyl group as the growing polymer chain. Furthermore, the energy of the titanium hydride system in the absence of any olefin was calculated, and it was found that the energy of the active site resting states with a propyl group are 41.4 and 33.6 kcal/mol lower in energy than the titanium hydride plus free propylene molecule system for the $TiCl_3$- and $TiCl_4$-based sites, respectively. Cavallo and co-workers considered this reaction for the $TiCl_3$-based Corradini site.[9] They were able to obtain a structure corresponding to a propene molecule bound to the hydride, but this structure was 26 kcal/mol higher in energy than the propyl resting state and insertion of the propene into the Ti−H bond was found to proceed with a barrier of only 0.3 kcal/mol.

It therefore must be concluded that for all sites insertion of an olefin into the Ti−H bond, the reverse reaction of β-elimination, has no or a very low barrier and is significantly exothermic. Therefore, it appears β-elimination is not a reasonable termination pathway given the present models of the active sites.

A number of papers have looked at termination via β-elimination in homogeneous catalysts (see for example refs 68−73). In general, these studies have givin similar conclusions to the present work. In ref 73 a number of cases were looked at, and it was found that the barrier to β-elimination was always higher than that to β-hydrogen transfer to a monomer but that the nature of the metal center and the steric environment around it can effect the height of the former barrier. It appears that although the Ti(III) and Ti(IV) sites are different electronically and in a steric environment, the combined effect of these two factors leads to high barriers to β-elimination and unstable metal hydride olefin complexes in both cases.

The reactant in the second chain transfer mechanism, β-hydrogen transfer to a monomer, is the active site with a π-complexed ethylene. The product is the active site with an ethyl group as the R group and a π-complexed α-olefin (propylene in this case). The transition state geometries and energies of the β-hydrogen transfer

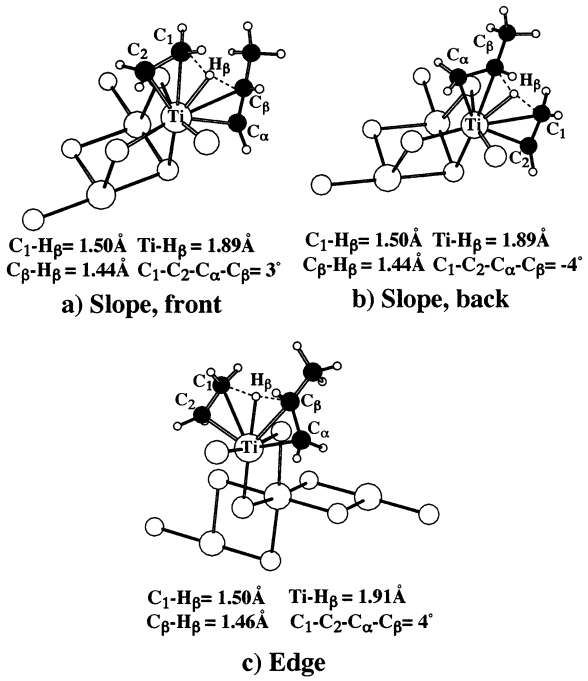

Figure 12. Chain transfer transition states of the $TiCl_4$-based sites.

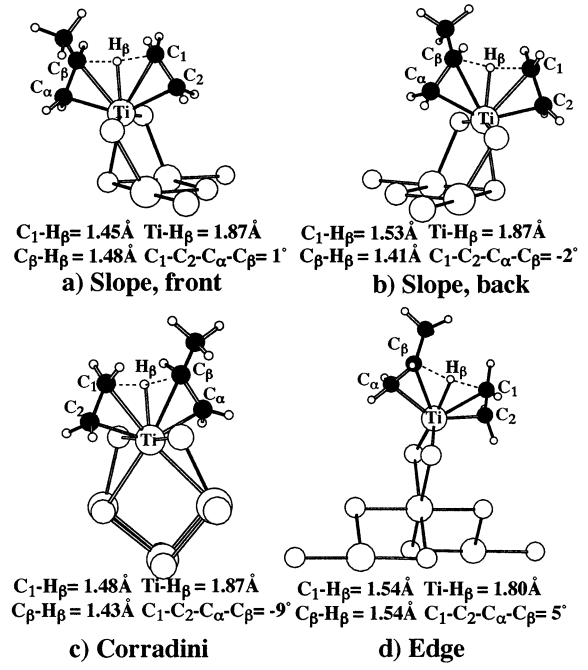

Figure 13. Chain transfer transition states of the $TiCl_3$-based sites.

reactions of all the sites under consideration were calculated. As was the case for the π-complexes and insertion transition states, for each of the edge and slope sites two termination transition states were considered corresponding to the monomer bound to the front and backsides of the active site. Also, following the insertion step reactions, the barriers to termination were calculated with respect to the π-complex ($E_{T(\pi)}$) and the separated ethylene and resting state ($E_{T(s)}$). The barriers and some important geometric parameters are given in Table 5, and the transition states are illustrated in Figures 12 and 13. It should be recalled that the barriers to chain transfer for the $TiCl_3$-based edge site "on $TiCl_2$" were calculated using a model of the surface that has

only one Ti atom with the rest of the cations being Mg atoms, like all of the "on $TiCl_2$" $TiCl_4$-based edge calculations and unlike the other $TiCl_3$-based edge site calculation "on $TiCl_2$".

From Figures 12 and 13 it is clear that the relative positioning of the polymer, H atom that is being transferred, and the monomer is the same in every transition state. The polymer and monomer are arranged in a trans fashion about the Ti atom with the H atom close to halfway between the C atoms of the polymer and the monomer and also quite close to the Ti atom. The geometrical requirements of this arrangement force some of the sites to distort significantly from the geometry of the π-complex. In the case of the $TiCl_3$-based slope sites the Cl−Ti−Cl angle formed by the bridging Cl atoms increases approximately 30°, creating enough space for either the polymer chain or the monomer to go between the two Cl atoms (Figure 13a,b). The presence of an extra ligand in the coordination sphere on the Ti atom in the $TiCl_4$-based slope site makes a similar distortion impossible. The transition state geometry of this site when ethylene binds from the front side (Figure 12a) has the olefin trans to the surface but pushed toward the bridging Cl atoms and the polymer chain forced relatively close to the surface. The Corradini site has a lot of space above it, particularly once the π-complex is formed, and therefore it has no trouble accommodating the steric demands of the transition state (Figure 13e). The same cannot be said for the edge site. Although the $TiCl_3$-based slope and edge sites have some similarities in terms of geometry, the edge site is unable to widen the angle between the bridging Cl atoms to accommodate the transition state because both of these atoms are bonded to the same surface cation. Instead, the Ti to surface Cl bond breaks to give the structure illustrated in Figure 13d. Alternative transition states where the Ti to surface Cl bond was retained were found, but these are more than 4 kcal/mol higher in energy than the transition state where the bond is broken. Unsurprisingly, the weak Ti to surface bond in the $TiCl_4$-based edge site also breaks, giving a similar transition state geometry (Figure 12c). Once the bond between the Ti and the surface Cl atom is broken, the "front" and "back" sides of the edge site are equivalent, and it is for this reason that only single structures for the edge site are given in Figures 12c and 13d.

Despite the relatively strict geometrical requirements, the reaction barriers to the H-transfer reaction in Table 5 are rather low. So low that in many cases they are similar in magnitude or lower than the insertion barriers for the same site. Obviously, any site for which the termination barrier is lower than or equal to the insertion barrier is not going to be a good site for polymerization. The internal termination energy barriers follow similar trends to the insertion barriers with respect to the relative energies of the barriers to frontside and backside termination. With the exception of the $TiCl_3$-based Corradini site the termination barriers for the sites on $TiCl_2$ are lower than for the equivalent sites on $MgCl_2$ when these barriers are measured with respect to the separated monomer and site.

Cavallo and co-workers also calculated the barrier for H-transfer to the monomer for the Corradini site.[9] Somewhat surprisingly, they obtained a value of 19.3 kcal/mol for the height of this barrier despite the geometry of the transition state being very similar to that found in the present study.

Table 6. Probability of Insertion of Ethylene at Each Site Model (*p*) and Number- and Weight-Average Molecular Weights of the Polymer Produced at Each Site[a]

site type		*p*	M_n	M_w
$MgCl_2$ surface				
$TiCl_4$	slope	0.821619	157	286
$TiCl_4$	edge	0.998214	15709	31390
$TiCl_3$	slope	0.829006	164	300
$TiCl_3$	Corradini	0.267678	38	49
$TiCl_3$	edge	0.999894	265742	531455
$TiCl_2$ surface				
$TiCl_4$	slope	0.950936	572	1115
$TiCl_4$	edge	0.951223	575	1122
$TiCl_3$	slope	0.000090	28	28
$TiCl_3$	Corradini	0.103712	31	35
$TiCl_3$	edge	0.363110	44	60

[a] Molecular weights in g/mol.

With both the insertion and termination barriers at hand it is possible to calculate what will be the average molecular weight of the polymer produced by each type of site. Note that although entropy effects are neglected in this analysis they are expected to be small.

The calculated insertion probability at each site and the number-average molecular weight and weight-average molecular weight of the polymer produced at that site are listed in Table 6. Note that another possible outcome of the reaction has not been considered. After a hydrogen atom has been transferred to the monomer, the product is another π-complex this time with an ethyl group and an α-olefin of some length. If the olefin is bound strongly enough to the Ti, then it may remain long enough for it to insert into the new Ti−R σ-bond or for the H atom to transfer back again. It has been assumed that the barrier to loss of the olefin is much lower than those of insertion or termination. For the $TiCl_4$-based sites this is likely to be a reasonable approximation (with the obvious exception of insertion from the front at the $TiCl_4$-based edge site on $MgCl_2$) as the π-complexation energies are only slightly exothermic or endothermic for these sites. Ethylene is bound to the $TiCl_3$-based sites by about 10 kcal/mol. However, desorption of ethylene is entropically favored by about 10 kcal/mol at 350 K and should therefore have a lower barrier than insertion when Gibbs free energies are considered.

It is clear from Table 6 that, in terms of catalytic ability, the sites investigated fall into three groups: (a) those that are reasonable catalysts (the edge sites on $MgCl_2$), (b) those that are very poor catalysts (the slope sites with the exception of the $TiCl_3$-based slope site on $TiCl_2$ and the $TiCl_4$-based edge site on $TiCl_2$), and (c) those that effectively do not catalyze olefin polymerization at all (the Corradini sites and the $TiCl_3$-based slope and edge sites on $TiCl_2$). Experimentally, the polymer molecular weights produced by $TiCl_4/MgCl_2$ Ziegler−Natta catalysts in the absence of H_2 often fall into a range between 10 000 and 10 000 000 g/mol.[74,75] The two edge sites on $MgCl_2$ are predicted to produce polymers with molecular weights in this range and as such are very good candidates for models of the real active sites.

The calculated molecular weights are very sensitive to the relative transition state energies, and a change of 2−3 kcal/mol, a value which is less than the expected accuracy of the computational method used here, corresponds to 2 orders of magnitude change in M_n. The

four sites that are "very poor" catalysts therefore should not be excluded completely from the list of possible models of the real sites. The three remaining sites can probably be excluded as models of the real active sites unless effects not taken into account make a large difference to the energetics of polymerization at these sites.

5. Conclusions

The aim of this study was to examine several of the active sites that are proposed to be present in the $TiCl_4/MgCl_2$ Ziegler−Natta catalysts and to try and determine which best describe the actual active sites present in these catalysts.

The low binding energies of $TiCl_4$ in the possible sites on the surface of $MgCl_2$ strongly suggest that that $TiCl_4$ does not simply bind to the undercoordinated surface Mg atoms as has generally been assumed. Models of the active site starting from $TiCl_4$ on a $MgCl_2$ surface therefore are probably unreasonable. The experimental studies of Somorjai and co-workers have found that Ti is present in several layers below the uppermost in their model catalyst.[30,59,60] The present calculations show that $TiCl_4$ binds more strongly to $MgCl_2$ when one or more of the Mg atoms is replaced with a Ti atom or to a $TiCl_2$ surface. Alternative surface models of this type therefore should be considered when trying to describe the behavior of these types of catalysts. $TiCl_3$ binds well to $MgCl_2$ and sites formed from this Ti species, and $MgCl_2$ cannot be excluded from the list of possible site models on the basis of site stability at least.

The examination of the polymerization mechanism at each site provided a number of insights. The resting states of the $TiCl_3$-based sites were all found to include a β-hydrogen agostic interaction while none of the resting states of the $TiCl_4$-based sites showed this interaction. The π-complexation energies of the $TiCl_4$-based sites are qualitatively different from those of the $TiCl_3$-based sites. In the former case the binding energies are slightly exothermic or slightly endothermic or no geometry corresponding to a bound ethylene molecule could be found at all while in the latter case the monomer has a significant binding energy of approximately 10 kcal/mol. The internal energy barriers to insertion of the ethylene molecule into the Ti−C bond were generally larger for the $TiCl_3$-based sites compared to the $TiCl_4$-based sites, but this is reversed if the barriers are calculated with respect to the separated ethylene molecule and active site. The geometries of all the transition states of the insertion reaction show the cyclobutane-like transition state predicted by the Cossee−Arlman mechanism[33,34,35] and also all show some kind of agostic interaction as suggested by Brookhart and Green.[36]

The β-hydrogen elimination and β-hydrogen transfer with ethylene termination mechanisms were considered. The former mechanism appears to be unlikely to occur as it was found to be significantly endothermic, and the reverse reaction, insertion of an α-olefin into a Ti−H bond, should proceed with little or no barrier. Hydrogen transfer with ethylene, on the other hand, should be a viable termination pathway as the energy barriers calculated for this process are similar in magnitude to the insertion barriers.

Using the calculated energy barriers, theoretical polymer molecular weights for each model site were derived. Only some of the edge sites give molecular weights that are similar to what is found experimentally.

In the introduction nine active site models were described where these models were combinations of three Ti species ($TiCl_4$, $TiCl_3$, and $TiCl_2$) and three places to which they can adsorb so the surface of $MgCl_2$. This number was later increased to 18 with the addition of surfaces including Ti atoms in place of Mg. Of these sites the six $TiCl_2$-based and the two $TiCl_4$-based Corradini sites were eliminated on geometrical grounds. The other two $TiCl_4$-based sites on $MgCl_2$ can also be eliminated as they are unstable, and the active site will not remain on the surface. The $TiCl_3$-based Corradini sites and the $TiCl_3$-based slope site on $TiCl_2$ also do not appear to be good models of the real active sites since the termination reaction at these sites has a lower barrier than the propagation reaction. Two further sites, the $TiCl_4$-based slope site on $TiCl_2$ and the $TiCl_3$-based slope site on $MgCl_2$, should also be poor catalysts since their energy barriers for propagation are only slightly lower than their termination energy barriers, and they should therefore only be capable of producing short chains of polyethylene. The remaining three sites, the $TiCl_4$-based edge site on $TiCl_2$ and the two $TiCl_3$-based edge sites, have properties more in line with what is expected of the active site in a $TiCl_4/MgCl_2$ Ziegler−Natta catalyst and therefore are the best models of these sites of all the possibilities considered here. These statements should be made with the following caveat: the calculated molecular weights are highly sensitive to the energy barriers and the expected errors in these quantities when using the present methods are of the order of 2−3 kcal/mol. As such, the conclusions with respect to which sites are good catalysts are not completely conclusive though they still strongly suggest that many of the proposed structures of the active sites, if present in the catalytic system, would not contribute significantly to production of polyethylene.

One aspect of the polymerization reaction that has not been dealt with in this study is the barrier to formation of the π-complex between the active site and ethylene. The size of this barrier relative to the barrier of its reverse reaction (loss of ethylene) and the barrier of the propagation reaction determines the overall kinetics of the reaction.[76] Bohm showed that if the barrier to olefin uptake is small relative to either of the two other barriers, then the reaction will be independent of the monomer concentration.[76] Conversely, if the barrier to ethylene uptake is large relative to the barriers to loss of the monomer and insertion, then the polymerization reaction will be first order in the monomer concentration. A number of studies have found that the rate of polymerization does depend of the monomer concentration (for example refs 2, 75, and 77−79). Given the wide range of π-complexation energies found for the various sites, it is possible that appropriate calculations will also give a range of uptake barriers allowing further discrimination between possible active site models. As has already been noted, the size of the barrier to loss of ethylene from the π-complex may also have an effect on the termination reaction. We believe that it is most likely that the barrier to ethylene loss is small, but this not certain. Clearly, energies of the active site plus monomer system as the monomer approaches the Ti atom to for the π-complex are of interest in the context of this work. Calculations aimed at evaluating these energies and thereby deriving the barriers to monomer

uptake and loss are presently in progress and will be the focus of a forthcoming publication.

Acknowledgment. We thank Randal Ford, Francis de Rege, and Jeff Vanderbilt for helpful discussions. We also thank the Eastman Chemical Co. for financial support.

References and Notes

(1) Boor, J. J. *Ziegler−Natta Catalysts and Polymerizations*; Academic Press: New York, 1979.
(2) Barbé, P. C.; Cecchin, G.; Noristi, L. *Adv. Polym. Sci.* **1987**, *81*, 1.
(3) Giunchi, G.; Clementi, E.; Ruiz-Vizcaya, M. E.; Novaro, O. *Chem. Phys. Lett.* **1977**, *49*, 8.
(4) Novaro, O.; Blaisten-Barojas, E.; Clementi, E.; Giunchi, G.; Ruiz-Vizcaya, M. E. *J. Chem. Phys.* **1978**, *58*, 2337.
(5) Fujimoto, H.; Yamasaki, T.; Mizutani, H.; Koga, N. *J. Am. Chem. Soc.* **1985**, *107*, 6157.
(6) Sakai, S. *J. Phys. Chem.* **1994**, *98*, 12053.
(7) Jensen, V. R.; Borve, K. J.; Ystenes, M. *J. Am. Chem. Soc.* **1995**, *117*, 9.
(8) Lin, J. S.; Catlow, C. R. A. *J. Catal.* **1995**, *157*, 145.
(9) Cavallo, L.; Guerra, G.; Corradini, P. *J. Am. Chem. Soc.* **1998**, *120*, 2428.
(10) Monaco, G.; Toto, M.; Guerra, G.; Corradini, P.; Cavello, L. *Macromolecules* **2000**, *33*, 8953.
(11) Gale, J. D.; Catlow, C. R. A.; Gillan, M. J. *Top. Catal.* **1999**, *9*, 235.
(12) Puhakka, E.; Pakkanen, T. T.; Pakkanen, T. A. *Surf. Sci.* **1995**, *334*, 289.
(13) Puhakka, E.; Pakkanen, T. T.; Pakkanen, T. A. *J. Mol. Catal. A* **1997**, *120*, 143.
(14) Shiga, A.; Kawamura-Kuribayashi, H.; Sasaki, T. *J. Mol. Catal. A* **1995**, *98*, 15.
(15) Boero, M.; Parrinello, M.; Terakura, K. *J. Am. Chem. Soc.* **1998**, *120*, 2746.
(16) Boero, M.; Parrinello, M.; Hüffer, S.; Weiss, H. *J. Am. Chem. Soc.* **2000**, *122*, 501.
(17) Boero, M.; Parrinello, M.; Weiss, H.; Hüffer, S. *J. Phys. Chem. A* **2001**, *105*, 5096.
(18) Weiss, H.; Boero, M.; Parinello, M. *Macromol. Symp.* **2001**, *173*, 137.
(19) Toto, M.; Morini, G.; Guerra, G.; Corradini, P.; Cavallo, L. *Macromolecules* **2000**, *33*, 1134.
(20) Giannini, U. *Makromol. Chem. Suppl.* **1981**, *4*, 216.
(21) Corradini, P.; Barone, V.; Fusco, R.; Guerra, G. *Gazz. Chim. Ital.* **1983**, *113*, 601.
(22) Mori, H.; Sawado, M.; Hasebe, T. H. K.; Nobuo; Terano, M. *Macromol. Rapid Commun.* **1999**, *20*, 245.
(23) Corradini, P.; Busico, V.; Guerra, G. *Compr. Polym. Sci.* **1988**, *4*, 29−50.
(24) Busico, V.; Cipullo, R.; Corradini, P.; De Biasio, R. *Macromol. Chem. Phys.* **1995**, *334*, 289.
(25) Chien, J. C.; Wu, J.-C.; Kuo, C.-I. *J. Polym. Sci., Polym. Chem. Ed.* **1982**, *20*, 2019.
(26) Kashiwa, N.; Yoshitake, J. *Makromol. Chem.* **1984**, *185*, 1133.
(27) Zakharov, V. A.; Makhtarulin, S. I.; Poluboyarov, V. A.; Anufrienko, V. F. *Makromol. Chem.* **1984**, *185*, 1781.
(28) Weber, S.; Chien, J. C. W.; Hu, Y. In *Transition Metals and Organometallics as Catalysts for Olefin Polymerization*; Kaminsky, W., Sinn, H., Eds.; Springer-Verlag: New York, 1988; pp 44−53.
(29) Brant, P.; Speca, A. N. *Macromolecules* **1987**, *20*, 2740.
(30) Magni, E.; Somorjai, G. A. *Catal. Lett.* **1995**, *35*, 205.
(31) Kissin, Y. V. *Makromol. Chem. Macromol. Symp.* **1993**, *66*, 83.
(32) Kissin, Y. V. *Makromol. Chem. Macromol. Symp.* **1995**, *89*, 113.
(33) Cossee, P. *J. Catal.* **1964**, *3*, 80.
(34) Arlman, E. *J. Catal.* **1964**, *3*, 89.
(35) Arlman, E.; Cossee, P. *J. Catal.* **1964**, *3*, 99.
(36) Brookhart, M.; Green, M. L. H. *J. Organomet. Chem.* **1983**, *395*, 250.
(37) Becke, A. D. *Phys. Rev. A* **1988**, *38*, 3098.
(38) Perdew, J. P. *Phys. Rev. B* **1986**, *33*, 8822.
(39) Vosko, S. H.; Wilk, L.; Nusair, M. *Can. J. Phys.* **1980**, *58*, 1200.
(40) ADF2000.01. Te Velde, G.; Bickelhaupt, F. M.; Baerends, E. J.; Fonseca Guerra, C.; Van Gisbergen, S. J. A.; Snijders, J. G.; Ziegler, T. *J. Comput. Chem.* **2001**, *22*, 931.
(41) Baerends, E. J.; Ellis, D. E.; Ros, P. *Chem. Phys.* **1973**, *2*, 41.
(42) Versluis, L.; Ziegler, T. *J. Chem. Phys.* **1988**, *88*, 322.
(43) Te Velde, G.; Baerends, E. J. *Phys. Rev. B* **1991**, *44*, 7888.
(44) Fonseca Guerra, C.; Snijders, J. G.; Te Velde, G.; Baerends, E. J. *Theor. Chim. Acta* **1998**, *99*, 391.
(45) Bagus, P. S.; Illas, F. In *The Encyclopedia of Computational Chemistry*; v. R. Schleyer, P., Allinger, N., Clark, T., Gasteiger, J., III, H. F. S., Schreiner, P. R., Eds.; John Wiley and Sons: Chichester, 1998; pp 2870−2887.
(46) BAND2000.01. Te Velde, G.; Baerends, E. J. *J. Comput. Phys.* **1992**, *99*.
(47) Blöchl, P. E. *Phys. Rev. B* **1994**, *50*, 17953.
(48) Car, R.; Parinello, M. *Phys. Rev. Lett.* **1985**, *55*, 2471.
(49) Krijn, J.; Baerends, E. J. *Fit Functions in the HFS Method*, Tech. Rep., Department of Theoretical Chemistry, Free University, Amsterdam, The Netherlands, 1984.
(50) Clark, M.; Cramer, R. D. I.; Van Opdenbosch, N. *J. Comput. Chem.* **1989**, *10*, 982.
(51) Rappé, A. K.; Casewit, C. J.; Colwell, K. S.; Goddard, W A, I.; Skiff, W. M. *J. Am. Chem. Soc.* **1992**, *114*, 10024.
(52) Wychoff, R. W. G. *Crystal Structures*, 2nd ed.; John Wiley and Sons: New York, 1963; Vol. 1.
(53) Magni, E.; Somorjai, G. A. *Appl. Surf. Sci.* **1995**, *89*, 187.
(54) Magni, E.; Somorjai, G. A. *J. Phys. Chem. B* **1998**, *102*, 8788.
(55) Chien, J. C.; Bres, P. *J. Polym. Sci., Polym. Chem. Ed.* **1989**, *27*, 1499.
(56) Fregonese, D.; Mortara, S.; Bresadola, S. *J. Mol. Catal. A* **2001**, *172*, 89.
(57) Jones, P. J. V.; Oldman, R. J. In *Transition Metals and Organometallics as Catalysts for Olefin Polymerization*; Kaminsky, W., Sinn, H., Eds.; Springer-Verlag: Berlin, 1988; pp 223−229.
(58) Potapov, A. G.; Kriventsov, V. V.; Kochubey, D. I.; Bukatov, G. D.; Zakharov, V. A. *Macromol. Chem. Phys.* **1997**, *198*, 3477.
(59) Magni, E.; Somorjai, G. A. *J. Phys. Chem.* **1996**, *100*, 14786.
(60) Kim, S. H.; Somorjai, G. A. *J. Phys. Chem. B* **2000**, *104*, 5519.
(61) Galli, P.; Luciani, L.; Cecchin, G. *Angew. Makromol. Chem.* **1981**, *94*, 63.
(62) Zakharov, V. A.; Makhtarulin, S. I.; Perkovets, D. V.; Moroz, E. M.; Mikenas, T. B.; Bukatov, G. D. *Stud. Surf. Sci. Catal.* **1986**, *25*, 71.
(63) Magni, E.; Somorjai, G. A. *Surf. Sci.* **1996**, *345*, 1.
(64) Albizzati, E.; Giannini, U.; Balbonti, G.; Camurati, I.; Chadwick, J. D.; Dall'occo, T.; Dubitsky, Y.; Galimberti, M.; Morini, G.; Maldotti, A. *J. Polym. Sci., Part A: Polym. Chem.* **1997**, *35*, 2645.
(65) Natta, G.; Pasquon, I. *Adv. Catal.* **1959**, *11*, 1.
(66) Machon, J. P.; Hermit, R.; Houzeaux, J. *J. Polym. Sci., Symp.* **1975**, 107.
(67) Chien, J. C.; Bres, P. *J. Polym. Sci., Polym. Chem. Ed.* **1986**, *24*, 1967.
(68) Woo, T. K.; Fan, L.; Ziegler, T. *Organometallics* **1994**, *13*, 2252.
(69) Sini, G.; McGregor, S. A.; Eisenstein, O.; Teuben, J. H. *Organometallics* **1994**, *13*, 1049.
(70) Yoshida, T.; Koga, N.; Morokuma, K. *Organometallics* **1995**, *14*, 746.
(71) Cavallo, L.; Guerra, G. *Macromolecules* **1996**, *29*, 2729.
(72) Woo, T. K.; Margl, P. M.; Ziegler, T.; Blöchl, P. *Organometallics* **1997**, *16*, 3454.
(73) Margl, P.; Deng, L.; Ziegler, T. *J. Am. Chem. Soc.* **1999**, *121*, 154.
(74) Chien, J. C.; Bres, P. *J. Polym. Sci., Polym. Chem. Ed.* **1986**, *24*, 2483.
(75) Kissin, Y. V.; Mink, R. I.; Nowlin, T. E. *J. Polym. Sci., Polym. Chem. Ed.* **1999**, *37*, 4255.
(76) Bohm, L. L. *Polymer* **1978**, *19*, 545.
(77) Bohm, L. L. *Polymer* **1978**, *19*, 553.
(78) Kissin, Y. V. *J. Mol. Catal.* **1989**, *46*, 220.
(79) Han-Adebkun, G. C.; Ray, W. H. *J. Appl. Polym. Sci.* **1997**, *65*, 1037.

MA0204554